Journal of Cerebral Blood Flow & Metabolism (2012) 32, 1589–1599

www.jcbfm.com

Effect of mild cognitive impairment and APOE genotype on resting cerebral blood flow and its association with cognition

Christina E Wierenga[1,2,3], Sheena I Dev[1], David D Shin[4], Lindsay R Clark[5], Katherine J Bangen[2], Amy J Jak[2,6], Robert A Rissman[7], Thomas T Liu[4], David P Salmon[7] and Mark W Bondi[2,6]

[1]*Research Service, Veterans Affairs San Diego Healthcare System, San Diego, California, USA;* [2]*Department of Psychiatry, School of Medicine, University of California San Diego, San Diego, California, USA;* [3]*Veterans Medical Research Foundation, San Diego, California, USA;* [4]*Department of Radiology, School of Medicine, University of California San Diego, San Diego, California, USA;* [5]*San Diego Joint Doctoral Program in Clinical Psychology, San Diego State University/University of California San Diego, San Diego, California, USA;* [6]*Psychology Service, Veterans Affairs San Diego Healthcare System, San Diego, California, USA;* [7]*Department of Neurosciences, School of Medicine, University of California San Diego, San Diego, California, USA*

Using whole-brain pulsed arterial spin labeling magnetic resonance imaging, resting cerebral blood flow (CBF) was measured in 20 mild cognitive impairment (MCI; 11 ε3 and 9 ε4) and 40 demographically matched cognitively normal (CN; 27 ε3 and 13 ε4) participants. An interaction of apolipoprotein (APOE) genotype (ε3 and ε4) and cognitive status (CN and MCI) on quantified gray-matter CBF corrected for partial volume effects was found in the left parahippocampal and fusiform gyri (PHG/FG), right middle frontal gyrus, and left medial frontal gyrus. In the PHG/FG, CBF was elevated for CN ε4 carriers but decreased for MCI ε4 carriers. The opposite pattern was seen in frontal regions: CBF was decreased for CN ε4 carriers but increased for MCI ε4 carriers. Cerebral blood flow in the PHG/FG was positively correlated with verbal memory for CN ε4 adults ($r = 0.67$, $P = 0.01$). Cerebral blood flow in the left medial frontal gyrus was positively correlated with verbal memory for MCI ε4 adults ($r = 0.70$, $P = 0.05$). Findings support dynamic pathophysiologic processes in the brain associated with Alzheimer's disease risk and indicate that cognitive status and APOE genotype have interactive effects on CBF. Correlations between CBF and verbal memory suggest a differential neurovascular compensatory response in posterior and anterior cortices with cognitive decline in ε4 adults.
Journal of Cerebral Blood Flow & Metabolism (2012) **32,** 1589–1599; doi:10.1038/jcbfm.2012.58; published online 2 May 2012

Keywords: apolipoprotein E; arterial spin labeling; cognition; mild cognitive impairment

Introduction

The independent contributions of cognitive and genetic risk factors for Alzheimer's disease (AD) have received considerable attention, but less is known about possible interactive effects. Mild cognitive impairment (MCI) is the most well-characterized cognitive risk factor for AD and is considered to be a transitional state between normal aging and dementia with rates of progression to AD reported to range between 16% and 40% (Marra *et al*, 2011). The apolipoprotein (APOE) ε4 allele is a well-known susceptibility gene for the development of late-onset AD, occurs in ~15% to 20% of the population, and is estimated to account for ~40% of AD cases (Devanand *et al*, 2005; Saunders *et al*, 1993). The APOE ε4 allele has been linked to AD neuropathology (e.g., increases in amyloid β deposition, dysregulation of tau phosphorylation), as well as small vessel arteriolosclerosis and microinfarcts of the deep nuclei in autopsy-confirmed patients with AD, suggesting that the allele also has deleterious

Correspondence: Dr CE Wierenga, UCSD Department of Psychiatry/VA San Diego Healthcare System, University of California, 3350 La Jolla Village Drive, Mailcode (151B), San Diego, CA 92161, USA.
E-mail: cwierenga@ucsd.edu
This work was supported by the Alzheimer's Association (NIRG 09-131856 to CEW and IIRG 07-59343 to MWB); VA CSR&D (CDA-2-022-08S to CEW); the National Institute on Aging (R01 AG012674 and K24 AG026431 to MWB); and the National Institutes of Health (1R01MH084796 to TTL).
Received 22 November 2011; revised 27 January 2012; accepted 1 March 2012; published online 2 May 2012

effects on cerebral microvascular integrity (Mahley *et al*, 1996; Morris *et al*, 2010; Tiraboschi *et al*, 2004; Yip *et al*, 2005).

A growing body of research indicates that functional brain changes precede structural decline in dementia risk, and changes in brain function have been reported both in asymptomatic cognitively intact genetically at-risk adults (i.e., APOE ε4 carriers) and in symptomatic adults diagnosed with MCI (see Wierenga and Bondi, 2007 for review). Functional changes in adults at genetic or cognitive risk typically involve increased functional magnetic resonance imaging (MRI) blood oxygen level-dependent (BOLD) response and reductions in metabolism and blood flow measured by fluorodeoxyglucose positron emission tomography and single-photon emission computed tomography imaging methods, respectively (Reiman *et al*, 1996; Wolf *et al*, 2003). The recent finding of *decreased* BOLD response in presymptomatic carriers of familial AD mutation but increased BOLD response in APOE ε4 carriers (albeit only four subjects) challenges the argument that increased BOLD is related to cognitive compensation (e.g., recruitment of additional neural resources indicating greater cognitive effort required to maintain performance at an equivalent level to healthy peers) and raises the possibility of an unidentified effect of the APOE allelic variant on cerebral vascular reactivity (Ringman *et al*, 2011). Since the BOLD signal reflects local changes in deoxyhemoglobin content, which in turn exhibits a complex dependence on changes in cerebral blood flow (CBF), cerebral blood volume, and the cerebral metabolic rate of oxygen consumption (Buxton *et al*, 2004), group differences in the BOLD response may also reflect variations in cerebrovascular functioning that become more pronounced with age or disease and can be confused with alterations in neural activity (D'Esposito *et al*, 2003). Therefore, direct assessment of CBF through perfusion imaging offers considerable promise as a noninvasive technique for detecting such early and oftentimes subtle functional brain changes that occur in preclinical or prodromal stages. In light of evidence of altered BOLD signal, the study of changes in resting gray-matter (GM) CBF in dementia risk may provide important information for early diagnosis, disease conversion, and monitoring of disease progression.

Reflecting the close relationship between blood perfusion and metabolism in the brain, alterations in CBF may also represent a precursor to cognitive decline in dementia risk. Cerebral blood flow refers to the rate of delivery of arterial blood to a capillary bed in brain tissue. Since CBF delivers glucose and oxygen to the brain, changes in CBF at rest may reflect not only a decrease in cerebrovascular integrity, but also altered neurovascular function that may affect cognition. Arterial spin labeling (ASL) MRI is a noninvasive cerebral perfusion method for the quantitative measurement of CBF. It uses an endogenous diffusible tracer by applying a magnetic label to the water molecules of flowing blood to invert the magnetization of the water in arterial blood before the blood reaches the image slice (Brown *et al*, 2007; Buxton, 2009). Typically, the ASL signal is then converted into a measure of CBF in absolute units (e.g., milliliters of blood/milliliter of tissue/minute—or milliliters of blood/100 g of tissue/minute) (Brown *et al*, 2007; Wong, 2005). An average value for CBF in GM of the adult brain is typically between 50 and 60 mL/100 g per minute. The quantitative CBF measurements from ASL are generally in agreement with other perfusion measurement techniques, although the CBF values with ASL tend to be slightly higher (Buxton, 2009; Ewing *et al*, 2005; Koziak *et al*, 2008). Methodologically, ASL techniques offer several advantages over fluorodeoxyglucose positron emission tomography and single-photon emission computed tomography methods of perfusion imaging in that they (1) are noninvasive and free of exposure to ionizing radiation, intravenous contrast agents, or radioactive isoforms, (2) are easily repeatable and can be performed within a short period of time (e.g., scans <10 minutes), (3) can be obtained during the same imaging session as structural or functional scans, (4) result in decreased intersubject and intersession variability, and (5) provide a quantitative measurement of CBF at rest and during brain activation. Therefore, ASL MRI has significant potential for application to the study of disease diagnosis and progression.

Given the recent advent of ASL, only a few published reports show its use in examining CBF alterations in adults at risk for AD. Results have been equivocal and adults with MCI have shown both increases and decreases in CBF across studies but also in the same subjects across different regions. For example, *decreased* CBF in MCI has been reported in the posterior cingulate (Dai *et al*, 2009), right inferior parietal lobe (Johnson *et al*, 2005), and right precuneus (Xu *et al*, 2007), whereas *increased* CBF has been reported in the medial temporal lobe, amygdala, anterior cingulate, and basal ganglia compared with cognitively intact peers (Dai *et al*, 2009). In contrast, adults with AD consistently tend to show widespread decreases in CBF compared with either normal control group or adults with MCI in the inferior parietal lobe extending to the posterior cingulate cortex, left lateral frontal lobe, left superior temporal region, and left orbitofrontal cortex (Alsop *et al*, 2000; Dai *et al*, 2009; Detre and Alsop, 1999; Johnson *et al*, 2005). Alterations of CBF appear largely independent of cortical GM atrophy (Johnson *et al*, 2005).

Despite clear implications for disease-related alterations in CBF on cognition, the relationship between resting CBF and cognition has not been comprehensively explored in aging, dementia risk, or AD. In an elegant longitudinal study by Chao *et al* (2010), resting CBF in the right inferior parietal lobe including the precuneus and the right middle frontal gyrus was associated with progression to dementia. Another study found a positive correlation between CBF in the right precuneus and memory performance

in cognitively normal (CN) adults and adults with MCI (Xu *et al*, 2007), suggesting that hypoperfusion negatively affects cognition. Together, these studies support a functional localization between resting CBF and cognition.

The present investigation addressed limitations of previous studies (e.g., partial brain coverage, lack of CBF quantification, and absence of associations between CBF and neuropsychological performance) and investigated the impact of genetic (APOE $\varepsilon 4$ allele) and cognitive (MCI) risk for AD on resting GM CBF and its associations with neuropsychological performance. The traditional CBF landscape in the healthy brain is characterized by hyperfrontality, indicating a regional difference whereby perfusion is greater to frontal regions than posterior regions (Parkes *et al*, 2004), and age-related GM perfusion declines are predominantly localized in the frontal cortex (Parkes *et al*, 2004). Against this backdrop, we hypothesized that dementia risk would result in altered CBF whereby (1) asymptomatic adults at genetic risk for AD (e.g., CN $\varepsilon 4$) would show elevated CBF in posterior regions and decreased CBF in anterior regions compared with CN $\varepsilon 3$ carriers, consistent with a compensatory brain response in regions implicated early in the AD process, (2) adults with MCI would show decreased CBF compared with CN peers in posterior cortices more susceptible to AD neuropathology, and this difference may be greater for symptomatic adults at genetic risk for AD (e.g., MCI $\varepsilon 4$) suggesting a more deleterious effect of genetic susceptibility in cognitively impaired adults. Additionally, we predicted that (3) CBF in regions of group difference would selectively correlate with neuropsychological performance in associated cognitive domains indicating functional localization of CBF changes (e.g., CBF in medial temporal lobe would correlate with memory performance) providing support for the notion of compensatory mechanisms.

Materials and methods

Participants

Twenty right-handed adults diagnosed with MCI and forty neurologically and CN elderly adults enrolled in a longitudinal study of healthy aging participated. The CN participants were recruited through newspaper advertisements and community lectures (i.e., no clinic-based or medical referral sources). All CN participants were considered to be normal based on the extensive medical, neurologic, laboratory, and neuropsychological evaluations. The MCI participants were recruited from the community and the UCSD Alzheimer's Disease Research Center. The CN participants included 27 $\varepsilon 3/\varepsilon 3$ homozygotes, 12 $\varepsilon 3/\varepsilon 4$ heterozygotes, and 1 $\varepsilon 4/\varepsilon 4$ homozygote. The MCI participants included 11 $\varepsilon 3/\varepsilon 3$ homozygotes, 6 $\varepsilon 3/\varepsilon 4$ heterozygotes, and 3 $\varepsilon 4/\varepsilon 4$ homozygotes. Because of the small number of $\varepsilon 4/\varepsilon 4$ homozygotes, gene dose effects were not examined. Participants with one or more $\varepsilon 2$ allele(s) were excluded due to allele's possible protective effects. Diagnosis of MCI was made independently by at least two neuropsychologists (AJ, CW, and MB) according to criteria put forth by Jak *et al* (2009). To strike a balance between the reliability and rigor of the diagnosis of MCI and sensitivity to detect mild impairment, performance on at least two tests within at least one cognitive domain falling 1 SD or more below their age-appropriate norms was required (see Heaton *et al*, 1991 for discussion of the use of 1 SD or more (and not 1.5 SD as suggested by Petersen) as the optimal standard score cutoff between normal and neurologic populations) in the absence of functional impairment. The MCI grouping comprised of four amnestic (one single domain and three multidomain) and seven nonamnestic (three single domain and four multidomain) $\varepsilon 3$ carriers and four amnestic (all single domain) and five nonamnestic (three single domain and two multidomain) $\varepsilon 4$ carriers. The groups based on APOE genotype ($\varepsilon 3$ and $\varepsilon 4$) did not differ in terms of MCI subtype ($\chi^2 = 5.3$, $P = 0.15$). Potential participants were excluded if they had dementia, a history of severe head injury, uncontrolled hypertension, the APOE $\varepsilon 2$ allele, or a Diagnostic and Statistical Manual of Mental Disorders-Fourth Edition Axis 1 diagnosis of learning disability, attention deficit disorder, mood disorder, or substance abuse. Persons with significant cerebrovascular disease, defined by Framingham Stroke Risk Profile (D'Agostino *et al*, 1994) 10-year probability of stroke $>30\%$, or a history of frank stroke or coronary artery disease were excluded. In addition, participants were excluded if they had contraindications to MRI scans such as metal in their body other than dental fillings, or if they were taking prescription psychoactive medications. No participant reported a significant level of depressive symptoms on the Geriatric Depression Scale (i.e., GDS >10).

The demographic characteristics and neuropsychological performances of the participants are shown in Table 1. The groups based on cognitive status (CN and MCI) did not differ in terms of age, gender distribution, or APOE $\varepsilon 4$ distribution. The groups also did not differ on indirect measures of vascular disease including GM CBF averaged across the whole brain, overall GM and white-matter (WM) volume, cerebrovascular health as indicated by percent stroke risk according to the Framingham Stroke Risk Profile, or pulse pressure (PP; the pulsatile component of blood pressure calculated from systole (SBP) and diastole (DBP)), fractional diastolic pressure (equal to PP/DBP), and fractional systolic pressure (equal to PP/SBP), which are related to coronary artery disease (Jankowski *et al*, 2004). However, the MCI group had slightly lower educational attainment than the CN group, though the sample as a whole is generally well educated. As expected, on the majority of neuropsychological tests, the MCI group performed worse than the CN group. Within cognitive groups, APOE $\varepsilon 4$ and APOE $\varepsilon 3$ carriers did not differ on any of these variables, with the exception that MCI APOE $\varepsilon 3$ carriers performed worse than APOE $\varepsilon 4$ carriers on the D-KEFS Color-Word Inhibition Switching condition ($P = 0.03$).

This research was approved by the Ethics Committee and Institutional Review Board at the University of California at San Diego and VA San Diego Healthcare System. Written informed consent was obtained from all

Table 1 Demographics and raw neuropsychological test scores of the CN and MCI groups

Variables	*Diagnosis*				
	CN, n = *40*		*MCI,* n = *20*		P *value*
	Mean	*(s.d.)*	*Mean*	*(s.d.)*	
Demographics					
Age (years)	73.5	(6.8)	74.8	(11.4)	0.63
Education (years)	16.3	(1.8)	14.5	(2.7)	0.01
Women/men	27	13	10	10	0.26
ε3/3; ε3/4; ε4/4	27;12;1		11;6;3		0.20
FSRP % stroke risk	11.0	(9.7)	12.5	(8.3)	0.58
Pulse pressure	50.0	(13.0)	51.8	(9.3)	0.68
Fractional diastolic pressure	0.66	(0.20)	0.68	(0.14)	0.76
Fractional systolic pressure	0.40	(0.08)	0.40	(0.05)	0.61
Whole-brain GM volume (mm^3)	581,863	(55,182)	551,196	(59,590)	0.06
Whole-brain WM volume (mm^3)	445,139	(52,293)	433,632	(56,121)	0.44
Whole-brain GM CBF (mL/100 g per minute)	53.6	(17.0)	55.7	(16.9)	0.27
Global cognition					
DRS total (out of 144)	142	(1.7)	136.3	(4.4)	< 0.01
Learning and memory					
WMS-R LM immediate recall	30.1	(6.6)	20.0	(5.3)	< 0.01
WMS-R LM delayed recall	28.0	(6.9)	15.4	(7.8)	< 0.01
CVLT-2 List 1–5 total	51.4	(11.8)	38.2	(9.3)	< 0.01
CVLT-2 SD free	10.9	(3.4)	6.7	(3.7)	< 0.01
CVLT-2 LD free	11.0	(3.6)	7.1	(3.5)	< 0.01
Language					
Animal Fluency	22.2	(5.1)	18.8	(6.4)	0.04
Letter Fluency (F,A,S)	47.2	(12.4)	37.9	(11.9)	< 0.01
DRS Supermarket items	28.0	(8.7)	22.6	(5.1)	0.01
Boston Naming Test	58.1	(2.4)	55.7	(3.3)	< 0.01
Executive function					
WAIS-R Digit Span Backwards	5.7	(1.2)	4.6	(1.3)	< 0.01
D-KEFS CW Inhibition	57.8	(10.6)	75.4	(17.8)	< 0.01
D-KEFS CW Inhibition/Switching	64.4	(14.2)	90.3	(40.5)	0.01
D-KEFS Trails Number-Letter Switching	80.6	(21.1)	130.8	(53.8)	< 0.01

GM, gray matter; WM, white matter; DRS, Dementia Rating Scale; FSRP, Framingham Stroke Risk Profile; WMS-R, Wechsler Memory Scale-Revised, LM, Logical Memory subtest; CVLT, California Verbal Learning Test; SD, short delay; LD, long delay; D-KEFS, Delis-Kaplan Executive Function System; CW, Color-Word; CBF, cerebral blood flow; MCI, mild cognitive impairment; CN, cognitively normal.

participants according to guidelines established by the Declaration of Helsinki.

Apolipoprotein E Genotyping

Genotyping for APOE alleles was performed using PCR restriction fragment length polymorphism analysis. Genomic DNA was collected from participants using buccal swab and extracted using Qiamp DNA blood mini kit (Qiagen, Valencia, CA, USA) followed by PCR amplification. The amplification reaction contained 5 μL genomic DNA, 2.5 units of Taq DNA Polymerase (New England Biolabs, Inc, Ipswich, MA, USA), 1 × ThermoPol Reaction Buffer (New England Biolabs), 0.3 mmol/L dNTPs, 10% DMSO, and 0.3 μmol/L of each primer (forward primer: 5′-ACGCGGGCACGGCTGTCCAAGGA-3′; reverse primer: 5′-GCGGGCCCCGGCCTGGTACAC-3′). The PCR cycling conditions were as follows: initial denaturation at 94°C for 3 minutes followed by 30 cycles of 94°C for 30 seconds and 72°C for 90 seconds with a final extension at 72°C for 4 minutes. Amplification was performed on a C1000 Thermocycler (BioRad Laboratories, Hercules, CA, USA). After PCR, the amplicon products were digested with 10 units of restriction enzyme *Hha*1 (New England Biolab) at 37°C for > 4 hours. The resulting DNA fragments were analyzed by separation on a 12% acrylamide gel. After electrophoresis, the gel was incubated in ethidium bromide and visualized under UV illumination.

Image Acquisition

Imaging data were acquired on a GE Signa Excite 3-T whole body system with a body transmit coil and an 8-channel receive-only head coil. A high-resolution T1-weighted 3D FSPGR scan was obtained to provide anatomic reference: 25 cm field of view, 256 × 192 matrix, repetition time = 8 ms, echo time = 3.1 ms, flip angle = 12°, T1 = 600 ms, bandwidth = 31.25 kHz, 172 1 mm sagittal slices.

To assess CBF differences across participants, three sequences were acquired to obtain an absolute CBF measurement. Resting brain blood perfusion was measured with pulsed ASL using a modified flow-sensitive alternating inversion recovery sequence with both presaturation pulses and PICORE QUIPSS 2 postinversion saturation pulses and a spiral readout with four interleaves to reduce signal dropout due to susceptibility effects (Liu and Wong, 2005; Wong *et al*, 1998). Imaging parameters of the ASL scan were 22×22 cm field of view, a 64×64 matrix, 3.2 ms echo time, 2,500 ms repetition time, postsaturation and inversion times of TI1 = 600 ms and TI2 = 1,600 ms, tag thickness 10 cm, tag to proximal slice gap 1 cm, 20 5 mm axial slices, and 40 volumes for 20 tag + control image pairs (Wong, 2005). A scan with the 90° excitation pulse turned off for the first eight repetitions was acquired to obtain the equilibrium magnetization of cerebrospinal fluid (CSF) (a 36-second scan with repetition time = 4 seconds, echo time = 3.4 ms, number of excitations (NEX) = 9). The CSF signal was used to estimate the equilibrium magnetization of blood, which in turn was used to convert the perfusion signal into calibrated CBF units (mL blood/100 mL tissue per minute). A 32-second minimum contrast scan was acquired using an eight-shot acquisition with repetition time = 2,000 ms, echo time = 11 ms, NEX = 2 to estimate the combined transmit and receive coil inhomogeneities (Brumm *et al*, 2010). The two images were averaged to create the minimum contrast image. The ASL image was then divided by the minimum contrast image to remove the effect of coil inhomogeneity during the CBF quantification step (Shin *et al*, 2012).

Data Processing and Analyses

Image processing was performed with Analysis of Functional NeuroImages (*AFNI*; afni.nimh. nih.gov), FMRIB Software Library (*FSL*, Oxford, UK), and locally created MatLab scripts. Each ASL data set was reconstructed using the SENSE algorithm (Pruessmann *et al*, 1999; Weiger *et al*, 2002) to reduce sensitivity to the modulations that occur between shots caused by physiological fluctuations or motion. An automated MatLab script was used to preprocess the ASL data using AFNI and FSL tools. The ASL time series was coregistered to the middle time point to minimize the effects of participant motion. For each subject, a mean ASL image was formed from the average difference of the control and tag images using surround subtraction to create an uncorrected perfusion time series, and slice timing delays were accounted for, making the inversion time (TI2) slice specific (Liu and Wong, 2005). This mean ASL image was then converted to absolute units of CBF (mL/100 *g* tissue per minute) using an estimate of the equilibrium magnetization of CSF as a reference signal (Chalela *et al*, 2000). This resulted in a calibrated perfusion value for each voxel. Skull stripping of the high-resolution T1-weighted image was performed using Brain Surface Extractor (Shattuck *et al*, 2001), shown to outperform other methods in older adults (Fennema-Notestine *et al*, 2006). Scans were manually edited to remove residual nonbrain material when necessary. Tissue segmentation was performed using FSL's FAST algorithm to define CSF, GM, and WM regions. The high-resolution T1-weighted image and partial volume segmentations were registered to ASL space, and partial volume segmentations were down-sampled to the resolution of the ASL data. To correct the CBF measures for partial volume effects and ensure that CBF values were not influenced by known decreased perfusion in WM or increased volume of CSF (e.g., Hermes *et al*, 2007 and Parkes *et al*, 2004), we used the method previously reported by Johnson *et al* (2005). These calculations assume that CSF has zero CBF and that CBF in GM is 2.5 times greater than that in WM. The following formula was used to compute partial volume corrected CBF signal intensities: $CBF_{corr} = CBF_{uncorr}/(GM + 0.4 \times WM)$. The CBF_{corr} and CBF_{uncorr} are corrected and uncorrected CBF values, respectively. The GM and WM are gray-matter and white-matter partial volume fractions, respectively. Information from the high-resolution structural image and the FAST (FSL Automated Segmentation Tool) was used to determine the tissue content of each perfusion voxel. Using AFNI, a 4.0-mm full-width, half-maximum Gaussian filter was applied to the CBF_{corr} data. Voxels with negative intensities were replaced with zero (Brown *et al*, 2003). The CBF_{corr} data were warped to standard Talairach space and resampled to a $4 \times 4 \times 4$ mm resolution grid. Data were then screened for data quality and outlying values deviating by >3 SDs of the mean were eliminated.

Quantified CBF corrected for partial volume effects was compared using a 2 group (CN and MCI) $\times$ 2 APOE genotype ($\varepsilon 3$ and $\varepsilon 4$) voxelwise analysis of variance. Type I error was controlled based on Monte Carlo simulation results using AFNI's *AlphaSim* set with a voxelwise α of 0.05. Based on an averaged GM mask created from all the participants, a minimum cluster volume threshold of 1,280 μL or 20 contiguous voxels was chosen and this threshold/volume combination protected a whole-brain probability of false positives of $P < 0.05$. Effect sizes were calculated according to the following equation: $\eta^2 = (t^2/(t^2 + df))$ where $t = t$-value and df = degrees of freedom.

Associations with Cognition

Associations between CBF in activated clusters resulting from the interaction of cognitive group and APOE genotype and neuropsychological composite scores were then examined for each subgroup with correlations. A Bonferroni correction was applied for each region to correct for multiple comparisons, and correlations were only considered as significant at $P < 0.016$ ($P = 0.05/3$ regions). Composite scores were created for three neuropsychological domains hypothesized to be related to GM CBF: memory, executive functions, and language. Composite scores were calculated for the entire sample using principal component analysis on raw scores from the following 12 tests with oblique rotation (direct oblimin): California Verbal Learning Test (List A Trials 1 to 5, short delay free recall, and long delay free recall), Wechsler Memory Scale-Revised (Logical Memory immediate and delayed recall), Delis-Kaplan Executive Function System (Color-Word Inhibition and Inhibition/Switching, Trailmaking Letter-Number Switching subtests), Wechsler Adult Intelligence Scale

Table 2 Summary of principal component analysis to extract neuropsychological composite scores for the entire sample

Neuropsychological test	*Rotated factor loadings*		
	Verbal memory	*Executive functions*	*Language*
CVLT Short Delay Free Recall	**0.91**	−0.07	0.14
CVLT List A Trials 1–5	**0.89**	−0.11	0.11
CVLT Long Delay Free Recall	**0.89**	−0.03	0.13
WMS-R Logical Memory Immediate Recall	**0.83**	−0.09	0.19
WMS-R Logical Memory Delayed Recall	**0.81**	−0.04	0.16
D-KEFS Color-Word Inhibition/Switching	0.04	**0.93**	−0.04
D-KEFS Color-Word Inhibition	0.10	**0.93**	0.01
WAIS-R Digit Span Backwards	0.26	**−0.48**	0.06
D-KEFS Trail Making Letter-Number Switching	−0.18	**0.53**	**−0.56**
Animal Fluency	0.09	−0.09	**0.79**
DRS Supermarket items	−0.01	0.02	**0.69**
Boston Naming Test	0.33	−0.01	**0.57**
Percentage of variance explained	33.1	19.0	15.4

CVLT, California Verbal Learning Test; WMS-R, Wechsler Memory Scale-Revised; DRS, Dementia Rating Scale; D-KEFS, Delis-Kaplan Executive Function System; WAIS-R, Wechsler Adult Intelligence Scale-Revised.
Note: Factor loadings over 0.40 appear in bold.

Digit Span Backwards condition, Mattis Dementia Rating Scale Supermarket fluency condition, the Boston Naming Test, and animal fluency. The Kaiser–Meyer–Olkin measure verified the sampling adequacy for the analysis, KMO = 0.68, and Bartlett's test of sphericity X^2 (66) = 496, $P < 0.01$, and indicated that correlations between items were sufficiently large for principal component analysis. An initial analysis was run to obtain eigenvalues for each component in the data. Three components had eigenvalues over Kaiser's criterion of 1 and in combination these three factors explained 67.5% of the variance. Table 2 shows the factor loading after rotation. The items that cluster on the same components suggest that component 1 represents verbal memory, component 2 represents executive functions, and component 3 represents language. The resulting factor scores from each principal component analysis were saved and submitted to correlation analyses. For regions showing a significant correlation between CBF and composite neuropsychological test scores, hierarchical linear regression models determined whether CBF accounted for additional variance in each composite score above and beyond age, education, and overall cognitive function as determined by total raw score on the Mattis Dementia Rating Scale. The first model contained age and education as independent variables. The second model added Dementia Rating Scale raw score, and the third model added CBF and tested whether the additional change in variance was significant.

Results

Interaction of Cognitive Status and Apolipoprotein in Dementia Risk

Whole-brain voxel-level GM CBF comparisons revealed an interaction of APOE genotype ($\varepsilon 3$ and $\varepsilon 4$) and cognitive status (CN and MCI) on quantified CBF corrected for partial volume effects in the following three regions: (1) left parahippocampal gyrus (PHG) extending to the fusiform gyrus (FG), (2) right middle frontal gyrus, and (3) left medial frontal gyrus extending to the anterior cingulate (see Table 3 and Figure 1). In the left PHG/FG, CBF was elevated for CN $\varepsilon 4$ carriers but decreased for MCI $\varepsilon 4$ carriers. The opposite pattern was seen in frontal regions: CBF was decreased for CN $\varepsilon 4$ carriers but increased for MCI $\varepsilon 4$ carriers. The MCI participants, collapsed across genotype, showed increased CBF in three clusters in the right superior temporal gyrus including the anterior temporal pole, Brodmann's area 22, and the posterior aspect extending to the supramarginal gyrus and inferior parietal lobe. A main effect of cognitive group was also found in the right hippocampus extending to the pulvinar region of the thalamus and the left superior frontal gyrus (Figure 2). No main effect of APOE genotype was found. These results suggest that, in the left PHG/FG showing a cognitive status by APOE genotype interaction, possession of one risk factor (either genetic or cognitive) results in elevated CBF but possession of both risk factors results in decreased CBF. However, the opposite pattern was revealed in frontal regions, though the interaction was largely driven by the contrast between CN and MCI $\varepsilon 4$ carriers (Figure 1).

Relationships Between Cerebral Blood Flow and Cognition in Dementia Risk

Increased CBF in the left PHG/FG resulting from the interaction of cognitive group and APOE genotype was only correlated with improved verbal memory and only for CN $\varepsilon 4$ adults using the Bonferroni adjusted α-level of $P < 0.01$ ($r = 0.67$, $P = 0.01$), and this association remained significant after controlling for age, education, and overall cognitive function as determined by Mattis Dementia Rating Scale total raw score ($r = 0.75$, $P = 0.01$). The addition of CBF to

Table 3 Clusters of significant interaction between cognitive status (CN, MCI) and APOE (ε3, ε4) for resting gray-matter CBF resulting from a whole-brain voxelwise two-way ANOVA

Direction of response	*Hemisphere*	*Subregion (Brodmann's area)*	*Volume (mm^3)*	*Coordinates of maximum intensity voxel*	*F for maximum intensity voxel*	*η^2 (mean ± s.e.m.)*
Interaction of cognitive status × APOE						
	L	C1. Parahippocampal gyrus and fusiform gyrus (36, 20)	2,752	46L, 25P, 12I	11.3	0.38 ± 0.02
	R	C2. Middle and superior frontal gyrus (10)	1,856	30R, 43A, 4S	13.6	0.41 ± 0.03
	L	C3. Medial frontal gyrus, anterior cingulate (32,10)	1,408	14L, 43A, 8S	10.5	0.36 ± 0.03
Main effect of cognitive status						
MCI > CN	R	C1. Superior temporal gyrus, supramarginal gyrus, inferior parietal lobe (22, 40, 42)	5,632	66R, 37P, 20S	24.2	0.44 ± 0.02
	R	C2. Superior temporal gyrus (22)	2,176	54R, 11A, 0	18.1	0.42 ± 0.03
	R	C3. Superior temporal gyrus, anterior temporal pole (38)	1,344	34R, 15A, 24I	10.7	0.35 ± 0.02
	R	C4. Hippocampus, thalamus (pulvinar)	1,344	14R, 37P, 12S	10.2	0.42 ± 0.03
	L	C5. Superior frontal gyrus (10)	1,344	18L, 55A, 24S	13.1	0.44 ± 0.04

L, left; R, right; A, anterior; P, posterior; S, superior; I, inferior; C, cluster; CBF, cerebral blood flow; MCI, mild cognitive impairment; CN, cognitively normal; APOE, apolipoprotein; ANOVA, analysis of variance.
Clusters shown survived our cluster threshold α-protection procedure ($P < 0.05$, volume $> 1{,}280\,mm^3$; see text for details).

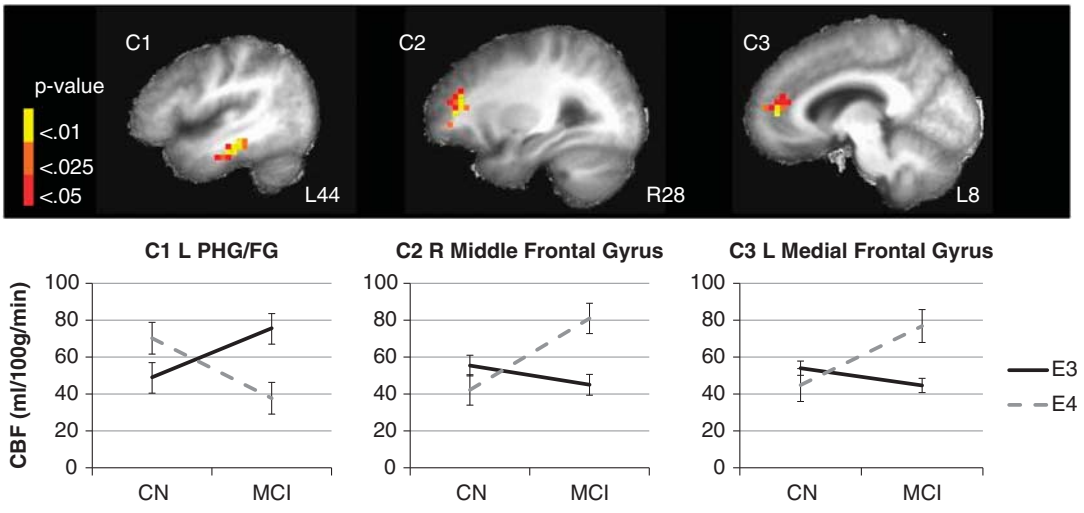

Figure 1 The interaction of cognitive status (CN and MCI) and APOE genotype (ε3 and ε4) on cerebral blood flow (CBF). Thresholded and clustered results (protecting a whole-brain voxelwise $P < 0.05$; red: $P < 0.05$, orange: $P < 0.025$, yellow: $P < 0.01$) for a two-way analysis of variance indicating an interaction of cognitive status (CN and MCI) and APOE genotype (ε3 and ε4) with corresponding graphical presentation of significant CBF differences. Error bars represent the standard error of the mean. Results are overlaid onto sagittal slices of a high-resolution anatomical image averaged across all participants (L: left; R: right; C: cluster; PHG/FG: parahippocampal gyrus/fusiform gyrus). For the interaction of cognitive status by APOE genotype: C1: CN ε3 = 46.0 ± 17.0, CN ε4 = 70.3 ± 45.5, MCI ε3 = 75.6 ± 43, MCI ε4 = 37.7 ± 12.7, $F(3,56) = 4.5$, $P < 0.01$; C2: CN ε3 = 64.1 ± 31.5, CN ε4 = 42.2 ± 18.8, MCI ε3 = 45.0 ± 17.4, MCI ε4 = 80.9 ± 33.6, $F(3,56) = 4.8$, $P < 0.01$; C3: CN ε3 = 58.9 ± 23.2, CN ε4 = 44.8 ± 11.8, MCI ε3 = 44.6 ± 14.6, MCI ε4 = 76.8 ± 40.3, $F(3,56) = 4.4$, $P < 0.01$. APOE, apolipoprotein; CN, cognitively normal; MCI, mild cognitive impairment.

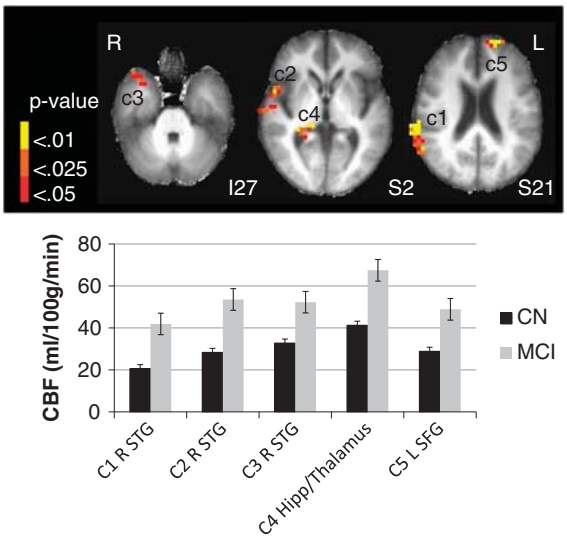

Figure 2 The effect of cognitive status on cerebral blood flow (CBF). Thresholded and clustered results (protecting a whole-brain voxelwise $P < 0.05$; red: $P < 0.05$, orange: $P < 0.025$, yellow: $P < 0.01$) for a two-way analysis of variance indicating a main effect of cognitive status (bottom right) with corresponding graphical presentation of significant CBF differences. Error bars represent the standard error of the mean. Results are overlaid onto axial slices of a high-resolution anatomical image averaged across all participants (L: left; R: right; I: inferior; S: superior; c: cluster; STG: superior temporal gyrus; Hipp: hippocampus). For main effect of cognitive status: C1: CN = 20.9 ± 8.7, MCI = 41.6 ± 18.5, $F(1,58) = 34.1$, $P < 0.001$; C2: CN = 29.5 ± 10.9, MCI = 53.2 ± 25.3, $F(1,58) = 25.4$, $P < 0.001$; C3: CN = 32.0 ± 13.6, MCI = 52.5 ± 20.3, $F(1,58) = 21.4$, $P < 0.001$; C4: CN = 41.7 ± 15.7, MCI = 67.2 ± 31.0, $F(1,58) = 17.8$, $P < 0.001$; C5: CN = 29.9 ± 12.0, MCI = 48.2 ± 20.0, $F(1,58) = 19.2$, $P < 0.001$. CN, cognitively normal; MCI, mild cognitive impairment; SFG, superior frontal gyrus.

a hierarchical linear regression model examining whether CBF in the left PHG/FG in CN $\varepsilon4$ adults explains a significant amount of variance in verbal memory above and beyond age, education, and overall cognitive function resulted in a significant change in R^2 ($\Delta R^2 = 0.50$, $\beta = 0.72$, $F(1,8)$ change = 10.5, $P = 0.01$, Cohen's $f^2 = 1.3$) and improved the significance of the overall model (i.e., from nonsignificant ($P = 0.74$) to a trend toward significance ($P = 0.07$)). Increased CBF in the left medial frontal gyrus was only correlated with better verbal memory and only for MCI $\varepsilon4$ adults ($r = 0.70$, $P = 0.05$), although this did not meet statistical significance after controlling for multiple comparisons. The correlations between CBF and verbal memory suggest a differential neurovascular compensatory response in cognitively intact and MCI APOE $\varepsilon4$ carriers, and raise the question of whether a shift from posterior to anterior cortices occurs with cognitive decline in $\varepsilon4$ adults. To fully test this hypothesis, longitudinal data and confirmation of AD neuropathology (e.g., decreased CSF amyloid β_{42}/tau ratio or increased amyloid β deposition in cortex) are needed.

Discussion

This study extended previous cerebral perfusion studies of aging and MCI to genetic risk and revealed an interaction between APOE genotype and cognitive status on CBF. Specifically, three regions were identified to be sensitive to the joint effects of cognitive and genetic risk for dementia on CBF, revealed by an interaction of APOE $\varepsilon4$ genotype and cognitive status in the left PHG extending to the FG, the right middle and superior frontal gyri, and the left medial frontal gyrus extending to the anterior cingulate. In the left PHG/FG, CBF was elevated for CN $\varepsilon4$ carriers but decreased for MCI $\varepsilon4$ carriers. The opposite pattern was seen in frontal regions: CBF was decreased for CN $\varepsilon4$ carriers but increased for MCI $\varepsilon4$ carriers. Associations between CBF alterations and neuropsychological performance were identified that support the relationship between CBF and cognition. Increased CBF in the left PHG/FG was correlated only with verbal memory for CN $\varepsilon4$ adults and accounted for a significant amount of the variance above age, education, and Dementia Rating Scale score. Increased CBF in the left medial frontal gyrus was only correlated with verbal memory for MCI $\varepsilon4$ adults.

Regional increases in CBF have been interpreted as indicating a cellular and vascular compensatory process in response to pathologic damage associated with incipient AD (Dai *et al*, 2009), whereas decreases in CBF are thought to reflect decreases in brain function. Neural activity results in increased blood flow (i.e., delivery of glucose and oxygen) and metabolism in the brain. Thus, since CBF supports cognitive function, increased blood flow may reflect increased demand for oxygen as a result of compensatory changes in the activity of neurons. In fact, it is this change in demand for energy that modulates CBF (Buxton, 2009). For example, the finding that, in APOE $\varepsilon4$ carriers, increased CBF in the left PHG/FG was correlated with verbal memory for CN adults and increased CBF in the left medial frontal gyrus was correlated with verbal memory for MCI adults suggests successful compensation and preservation of function in posterior regions affected early in the AD process before cognitive symptoms are evident. In adults with cognitive symptoms already present (e.g., suggestion of disease progression), anterior regions have a larger role. Moreover, the reduced CBF in the MCI $\varepsilon4$ group in the left PHG/FG reflecting a decreased ability to deliver oxygen, possibly resulting from changes in the neurovascular unit due to disease, is consistent with the speculated role of the APOE $\varepsilon4$ allele in blood–brain barrier alterations.

Correlations between CBF and verbal memory suggest a differential neurovascular compensatory response in frontal and posterior cortices in cognitively intact and MCI APOE $\varepsilon4$ carriers, respectively. Results suggest that, in posterior regions that appear more susceptible to early disease pathology, possession of one risk factor (APOE $\varepsilon4$ or MCI) results in elevated CBF but possession of both risk factors

results in decreased CBF, possibly due to greater likelihood of dementia conversion in adults with multiple risk factors. This result is consistent with Chao *et al*'s (2010) finding that posterior CBF (e.g., inferior parietal lobe) predicts dementia progression. The opposite pattern seen in the right middle frontal gyrus and left medial frontal gyrus (e.g., greater CBF for MCI APOE ε4) is consistent with the compensatory recruitment hypothesis suggesting increased reliance on frontal regions to compensate for a declining posterior hippocampal-parietal system (Cabeza *et al*, 2002; Daselaar *et al*, 2006). When interpreted within the context of prior studies reporting a lack of association between APOE ε4 and CBF in mild AD (Sakamoto *et al*, 2003) and MCI/AD combined (Luckhaus *et al*, 2010), and reports that nondemented older ε4 adults show greater CBF decline over 8 years measured with positron emission tomography (Thambisetty *et al*, 2010), these results suggest that the APOE ε4 allele may have the strongest impact on CBF during the transitional period between normal cognition and AD. This possibility is further supported by the lack of a main effect of APOE genotype on resting GM CBF. However, when collapsed across APOE genotype, our study confirmed prior brain imaging results revealing elevated CBF in MCI in several regions of the right superior temporal gyrus (including the anterior temporal pole, Brodmann's area 22, and a posterior aspect extending to the supramarginal gyrus and inferior parietal lobe), right hippocampus extending to the pulvinar nucleus of the thalamus, and the left superior frontal gyrus. This suggests that some regions may be more susceptible to perfusion changes that accompany MCI regardless of APOE genotype.

Taken together, our findings suggest that the transition from normal cognition to presumptive AD is likely associated with dynamic pathophysiologic changes in the brain and provide further support for a vascular role in AD risk. Findings reveal localized effects of CBF on domains of cognition, indicating differential involvement of regionally specific CBF changes on cognition. This specificity of CBF with respect to brain regions and cognition is valuable to better characterize changes in structure–function relationships in dementia risk. Our results are generally consistent with a compensatory response to overcome pathologic encroachments and reveal early changes in CBF in regions corresponding to the progression of the neuropathological changes of AD (i.e., early involvement of medial temporal lobe structures such as the hippocampus and entorhinal cortex to later involvement of frontal, temporal, and parietal cortices; Braak and Braak, 1991).

In conclusion, this study has several strengths, including whole-brain voxelwise CBF comparisons in a neuropsychologically well-characterized sample with associations between CBF and cognitive performance using partial volume corrected quantitative ASL MRI. These strengths set the current study apart from some of the large-scale efforts that, despite their large sample sizes and impressive statistical power, are limited in the variables they use to examine brain–behavior relationships. Smaller studies, such as this one, allow for sophisticated cognitive and imaging work-ups that ultimately may serve as seedbeds for hypothesis testing in next generation large-scale studies. Despite these strengths, there are several remaining limitations of ASL techniques. For instance, ASL has reduced sensitivity to weak activation because the overall magnetic resonance signal caused by the delivered arterial blood is only ~1% of the total signal due to the tissue resulting in a low intrinsic perfusion signal-to-noise ratio of pulsed ASL compared with that of exogenous tracers (e.g., xenon; Liu and Brown, 2007). ASL also relies on several assumptions in the perfusion quantification (e.g., tagging efficiency and transit delay). Transit delay sensitivity is a known issue affecting all ASL techniques that use a single inversion time. However, there are several drawbacks of using transit delay mapping techniques that are currently available, which limit our ability to apply them to a patient population, e.g., (1) they generally are more time consuming and (2) their sensitivity to perfusion is lower per unit acquisition time. Nevertheless, because our CBF measurements were derived from a population with similar demographics and cerebrovascular health, it is likely that that transit delay effects had equal influence on the conditions we investigated. Since transit delay sensitivity can be greatly reduced by increasing postlabeling delay, recent advances in pseudocontinuous ASL technique may hold promise in future studies as it can accommodate longer postlabeling delay (thanks to its ability to define larger temporal bolus relative to pulsed ASL) while preserving sufficient perfusion signal for accurate and reliable CBF measures (Shin *et al*, 2012). Results support the potential role for CBF measurement using ASL as a candidate biomarker for detecting early changes in the central nervous system associated with AD risk, as ASL offers the practical advantages of being noninvasive, relatively easy to implement compared with other functional imaging methodologies, and allows the ability to repeat scans to monitor longitudinal change.

Disclosure/conflict of interest

The authors declare no conflict of interest.

References

Alsop DC, Detre JA, Grossman M (2000) Assessment of cerebral blood flow in Alzheimer's disease by spin-labeled magnetic resonance imaging. *Ann Neurol* 47: 93–100

Braak H, Braak E (1991) Neuropathological staging of Alzheimer-related changes. *Acta Neuropathol (Berl)* 82: 239–59

Brown GG, Clark C, Liu TT (2007) Measurement of cerebral perfusion with arterial spin labeling: Part 2. Applications. *J Int Neuropsychol Soc* 13:526–38

Brown GG, Eyler Zorrilla LT, Georgy B, Kindermann SS, Wong EC, Buxton RB (2003) BOLD and perfusion response to finger-thumb apposition after acetazolamide administration: differential relationship to global perfusion. *J Cereb Blood Flow Metab* 23:829–37

Brumm KP, Perthen JE, Liu TT, Haist F, Ayalon L, Love T (2010) An arterial spin labeling investigation of cerebral blood flow deficits in chronic stroke survivors. *Neuroimage* 51:995–1005

Buxton RB (2009) *Introduction to functional magnetic resonance imaging: principles and techniques*. Cambridge: University Press

Buxton RB, Uludag K, Dubowitz DJ, Liu TT (2004) Modeling the hemodynamic response to brain activation. *Neuroimage* 23(Suppl 1):S220–33

Cabeza R, Anderson ND, Locantore JK, McIntosh AR (2002) Aging gracefully: compensatory brain activity in high-performing older adults. *Neuroimage* 17:1394–402

Chalela JA, Alsop DC, Gonzalez-Atavales JB, Maldjian JA, Kasner SE, Detre JA (2000) Magnetic resonance perfusion imaging in acute ischemic stroke using continuous arterial spin labeling. *Stroke* 31:680–7

Chao LL, Buckley ST, Kornak J, Schuff N, Madison C, Yaffe K, Miller BL, Kramer JH, Weiner MW (2010) ASL perfusion MRI predicts cognitive decline and conversion from MCI to dementia. *Alzheimer Dis Assoc Disord* 24:19–27

D'Agostino RB, Wolf PA, Belanger AJ, Kannel WB (1994) Stroke risk profile: adjustment for antihypertensive medication. The Framingham Study. *Stroke* 25:40–3

Dai W, Lopez OL, Carmichael OT, Becker JT, Kuller LH, Gach HM (2009) Mild cognitive impairment and Alzheimer's disease: patterns of altered cerebral blood flow at MR imaging. *Radiology* 250:856–66

Daselaar SM, Fleck MS, Dobbins IG, Madden DJ, Cabeza R (2006) Effects of healthy aging on hippocampal and rhinal memory functions: an event-related fMRI study. *Cereb Cortex* 16:1771–82

D'Esposito M, Deouell LY, Gazzaley A (2003) Alterations in the BOLD fMRI signal with ageing and disease: a challenge for neuroimaging. *Nat Rev Neurosci* 4:863–72

Detre JA, Alsop DC (1999) Perfusion magnetic resonance imaging with continuous arterial spin labeling: methods and clinical applications in the central nervous system. *Eur J Radiol* 30:115–24

Devanand DP, Pelton GH, Zamora D, Liu X, Tabert MH, Goodkind M, Scarmeas N, Braun I, Stern Y, Mayeux R (2005) Predictive utility of apolipoprotein E genotype for Alzheimer disease in outpatients with mild cognitive impairment. *Arch Neurol* 62:975–80

Ewing JR, Cao Y, Knight RA, Fenstermacher JD (2005) Arterial spin labeling: validity testing and comparison studies. *J Magn Reson Imaging* 22:737–40

Fennema-Notestine C, Ozyurt IB, Clark CP, Morris S, Bischoff-Grethe A, Bondi MW, Jernigan TL, Fischl B, Segonne F, Shattuck DW, Leahy RM, Rex DE, Toga AW, Zou KH, Brown GG (2006) Quantitative evaluation of automated skull-stripping methods applied to contemporary and legacy images: effects of diagnosis, bias correction, and slice location. *Hum Brain Mapp* 27: 99–113

Heaton RK, Grant I, Matthews CG (1991) *Comprehensive norms for an extended Halstead-Reitan neuropsychological battery: demographic corrections, research findings, and clinical applications*. Odessa, FL: Psychological Assessment Resources, Inc.

Hermes M, Hagemann D, Britz P, Lieser S, Rock J, Naumann E, Walter C (2007) Reproducibility of continuous arterial spin labeling perfusion MRI after 7 weeks. *MAGMA* 20:103–15

Jak AJ, Bondi MW, Delano-Wood L, Wierenga C, Corey-Bloom J, Salmon DP, Delis DC (2009) Quantification of five neuropsychological approaches to defining mild cognitive impairment. *Am J Geriatr Psychiatry* 17: 368–375

Jankowski P, Kawecka-Jaszcz K, Bryniarski L, Czarnecka D, Brzozowska-Kiszka M, Posnik-Urbanska A, Kpoec G, Dragan J, Klecha A, Dudek D (2004) Fractional diastolic and systolic pressure in the ascending aorta are related to the extent of coronary artery disease. *Am J Hypertens* 17:641–6

Johnson NA, Jahng GH, Weiner MW, Miller BL, Chui HC, Jagust WJ, Gorno-Tempini ML, Schuff N (2005) Pattern of cerebral hypoperfusion in Alzheimer disease and mild cognitive impairment measured with arterial spin-labeling MR imaging: initial experience. *Radiology* 234: 851–9

Koziak AM, Winter J, Lee TY, Thompson RT, St Lawrence KS (2008) Validation study of a pulsed arterial spin labeling technique by comparison to perfusion computed tomography. *Magn Reson Imaging* 26:543–53

Liu TT, Brown GG (2007) Measurement of cerebral perfusion with arterial spin labeling: Part 1. Methods. *J Int Neuropsychol Soc* 13:517–25

Liu TT, Wong EC (2005) A signal processing model for arterial spin labeling functional MRI. *Neuroimage* 24: 207–15

Luckhaus C, Cohnen M, Flüss MO, Jänner M, Grass-Kapanke B, Teipel SJ, Grothe M, Hampel H, Peters O, Kornhuber J, Maier W, Supprian T, Gaebel W, Mödder U, Wittsack HJ (2010) The relation of regional cerebral perfusion and atrophy in mild cognitive impairment (MCI) and early Alzheimer's dementia. *Psychiatry Res* 183:44–51

Mahley RW, Nathan BP, Pitas RE (1996) Apolipoprotein E. Structure, function, and possible roles in Alzheimer's disease. *Ann N Y Acad Sci* 777:139–45

Marra C, Ferraccioli M, Vita MG, Quaranta D, Gainotti G (2011) Patterns of cognitive decline and rates of conversion to dementia in patients with degenerative and vascular forms of MCI. *Curr Alzheimer Res* 8:24–31

Morris JC, Roe CM, Xiong C, Fagan AM, Goate AM, Holtzman DM, Mintun MA (2010) APOE predicts amyloid-beta but not tau Alzheimer pathology in cognitively normal aging. *Ann Neurol* 67:122–31

Parkes LM, Rashid W, Chard DT, Tofts PS (2004) Normal cerebral perfusion measurements using arterial spin labeling: reproducibility, stability, and age and gender effects. *Magn Reson Med* 51:736–43

Pruessmann KP, Weiger M, Scheidegger MB, Boesiger P (1999) SENSE: sensitivity encoding for fast MRI. *Magn Reson Med* 42:952–62

Reiman EM, Caselli RJ, Yun LS, Chen K, Bandy D, Minoshima S, Thibodeau SN, Osborne D (1996) Preclinical evidence of Alzheimer's disease in persons homozygous for the epsilon 4 allele for apolipoprotein E. *N Engl J Med* 334:752–8

Ringman JM, Medina LD, Braskie M, Rodriguez-Agudelo Y, Geschwind DH, Macias-Islas MA, Cummings JL, Bookheimer S (2011) Effects of risk genes on BOLD activation in presymptomatic carriers of familial Alzheimer's disease mutations during a novelty encoding task. *Cereb Cortex* 21:877–83

Sakamoto S, Matsuda H, Asada T, Ohnishi T, Nakano S, Kanetaka H, Takasaki M (2003) Apolipoprotein E genotype and early Alzheimer's disease: a longitudinal SPECT study. *J Neuroimaging* 13:113–23

Saunders AM, Strittmatter WJ, Schmechel D, George-Hyslop PH, Pericak-Vance MA, Joo SH, Rosi BL, Gusella JF, Crapper-MacLachlan DR, Alberts MJ *et al* (1993) Association of apolipoprotein E allele epsilon 4 with late-onset familial and sporadic Alzheimer's disease. *Neurology* 43:1467–72

Shattuck DW, Sandor-Leahy SR, Schaper KA, Rottenberg DA, Leahy RM (2001) Magnetic resonance image tissue classification using a partial volume model. *Neuroimage* 13:856–76

Shin DD, Liu TT, Wong EC, Shankaranarayanan A, Jung Y (2012) Pseudocontinuous arterial spin labeling with optimized tagging efficiency. *Magn Reson Med* doi: 10.1002/mrm.24113 (E-pub ahead of print 3 January 2012).

Thambisetty M, Beason-Held L, An Y, Kraut MA, Resnick SM (2010) APOE epsilon 4 genotype and longitudinal changes in cerebral blood flow in normal aging. *Arch Neurol* 67:93–8

Tiraboschi P, Hansen LA, Masliah E, Alford M, Thal LJ, Corey-Bloom J (2004) Impact of APOE genotype on neuropathologic and neurochemical markers of Alzheimer disease. *Neurology* 62:1977–83

Weiger M, Pruessmann KP, Osterbauer R, Bornert P, Boesiger P, Jezzard P (2002) Sensitivity-encoded single-shot spiral imaging for reduced susceptibility artifacts in BOLD fMRI. *Magn Reson Med* 48:860–866

Wierenga CE, Bondi MW (2007) Use of functional magnetic resonance imaging in the early identification of Alzheimer's disease. *Neuropsychol Rev* 17:127–43

Wolf H, Jelic V, Gertz HJ, Nordberg A, Julin P, Wahlund LO (2003) A critical discussion of the role of neuroimaging in mild cognitive impairment. *Acta Neurol Scand Suppl* 179:52–76

Wong EC (2005) Quantifying CBF with pulsed ASL: technical and pulse sequence factors. *J Magn Reson Imaging* 22:727–31

Wong EC, Buxton RB, Frank LR (1998) Quantitative imaging of perfusion using a single subtraction (QUIPSS and QUIPSS II). *Magn Reson Med* 39:702–8

Xu G, Antuono PG, Jones J, Xu Y, Wu G, Ward D, Li SJ (2007) Perfusion fMRI detects deficits in regional CBF during memory-encoding tasks in MCI subjects. *Neurology* 69:1650–6

Yip AG, McKee AC, Green RC, Wells J, Young H, Cupples LA, Farrer LA (2005) APOE, vascular pathology, and the AD brain. *Neurology* 65:259–65